State of the science in reconciling top-down and bottom-up approaches for terrestrial CO 2 budget

Masayuki Kondo, Prabir Patra, Stephen Sitch, Pierre Friedlingstein, Benjamin Poulter, Frederic Chevallier, Philippe Ciais, Josep Canadell, Ana Bastos, Ronny Lauerwald, et al.

PROF. MASAYUKI KONDO (Orcid ID : 0000-0001-5466-4847)
DR. BENJAMIN POULTER (Orcid ID : 0000-0002-9493-8600)
DR. VANESSA HAVERD (Orcid ID : 0000-0003-4359-5895)
DR. ATUL JAIN (Orcid ID : 0000-0002-4051-3228)
DR. ETSUSHI KATO (Orcid ID : 0000-0001-8814-804X)
DR. MARKUS KAUTZ (Orcid ID : 0000-0001-8763-3262)
DR. RACHEL M. LAW (Orcid ID : 0000-0002-7346-0927)
DR. DANICA LOMBARDOZZI (Orcid ID : 0000-0003-3557-7929)
DR. DAN ZHU (Orcid ID : 0000-0002-5857-1899)

Article type : Opinion

Prof. MASAYUKI KONDO (Orcid ID: 0000-0001-5466-4847)
Article type: Opinion

State of the science in reconciling top-down and bottom-up approaches for terrestrial CO_2 budget

Running Title: On reconciliation of CO_2 budgets

Masayuki Kondo[1,*], Prabir K. Patra[1,2], Stephen Sitch[3], Pierre Friedlingstein[4], Benjamin Poulter[5], Frederic Chevallier[6], Philippe Ciais[6], Josep G. Canadell[7], Ana Bastos[8], Ronny Lauerwald[9], Leonardo Calle[10], Kazuhito Ichii[1,11], Peter Anthoni[12], Almut Arneth[12], Vanessa Haverd[13], Atul K. Jain[14], Etsushi Kato[15], Markus Kautz[12, 16], Rachel M. Law[17], Sebastian Lienert[18], Danica Lombardozzi[19], Takashi Maki[20], Takashi Nakamura[21], Philippe Peylin[6], Christian Rödenbeck[22], Zhuravlev Ruslan[23], Tazu Saeki[11], Hanqin Tian[24], Dan Zhu[6], Tilo Ziehn[17]

[1]Center for Environmental Remote Sensing, Chiba University, Chiba 263-8522, Japan

[2]Department of Environmental Geochemical Cycle Research, Japan Agency for Marine–Earth Science and Technology, Yokohama 236-0001, Japan

[3]College of Life and Environmental Sciences, University of Exeter, Exeter EX4 4QF, UK

[4]College of Engineering, Mathematics and Physical Sciences, University of Exeter, Exeter EX4 4QF, UK

[5]National Aeronautics and Space Administration Goddard Space Flight Center, Biospheric Science Laboratory, Greenbelt, MD 20771, USA

[6]Laboratoire des Sciences du Climat et de l'Environnement, Institut Pierre Simon Laplace, 91191 Gif-sur-Yvette, France

[7]Global Carbon Project, Commonwealth Scientific and Industrial Research Organisation–Oceans and Atmosphere, Canberra, ACT 2601, Australia

[8]Department of Geography, Ludwig–Maximilians University of Munich, 80333 Munich, Germany

[9]Université Libre de Bruxelles, 1050 Bruxelles, Belgium

[10]W.A. Franke College of Forestry & Conservation, University of Montana, Missoula, MT 59812, USA

[11]Center for Global Environmental Research, National Institute for Environmental Studies, Tsukuba 305-8506, Japan

[12]Institute of Meteorology and Climate Research/Atmospheric Environmental Research, Karlsruhe Institute of Technology, 82467 Garmisch–Partenkirchen, Germany

[13]Commonwealth Scientific and Industrial Research Organisation–Oceans and Atmosphere, Canberra, ACT 2601, Australia

[14]Department of Atmospheric Sciences, University of Illinois at Urbana–Champaign, Urbana, IL 61801, USA

[15]Institute of Applied Energy, Tokyo, 105-0003, Japan

[16]Department of Forest Health, Forest Research Institute Baden-Württemberg, 79100 Freiburg, Germany

[17]Commonwealth Scientific and Industrial Research Organisation–Oceans and Atmosphere, Aspendale, VIC, Australia

[18]Climate and Environmental Physics, Physics Institute and Oeschger Centre for Climate Change Research, University of Bern, Bern, Switzerland

[19]Climate and Global Dynamics, National Center for Atmospheric Research, Boulder, CO 80305, USA

[20]Meteorological Research Institute, Tsukuba 305-0052, Japan

[21]Japan Meteorological Agency, Tokyo 100-8122, Japan

[22]Max Planck Institute for Biogeochemistry, 07745 Jena, Germany

[23]Central Aerological Observatory of Russian Hydromet Service, 141700, Russia

[24]International Center for Climate and Global Change Research, School of Forestry and Wildlife Sciences, Auburn University, Auburn, AL 36849, USA

***Correspondence:**

Masayuki Kondo

Center for Environmental Remote Sensing (CEReS), Chiba University

1-33 Yayoi-cho, Inage-ku, Chiba 263-8522, Japan

Tel/Fax: +81-43-290-3860

E-mail: Mkondo@chiba-u.jp

Abstract

Robust estimates of CO_2 budget, CO_2 exchanged between the atmosphere and terrestrial biosphere, are necessary to better understand the role of the terrestrial biosphere in mitigating anthropogenic CO_2 emissions. Over the past decade, this field of research has advanced through understanding of the differences and similarities of two fundamentally different approaches: "top-down" atmospheric inversions and "bottom-up" biosphere models. Since the first studies were undertaken, these approaches have shown an increasing level of agreement, but disagreements in some regions still persist, in part because they do not estimate the same quantity of atmosphere-biosphere CO_2 exchange. Here we conducted a thorough comparison of CO_2 budgets at multiple scales and from multiple methods to assess the current state of the science in estimating CO_2 budgets. Our set of atmospheric inversions and biosphere models, which were adjusted for a consistent flux definition, showed a high level of agreement for global and hemispheric CO_2 budgets in the 2000s. Regionally, improved agreement in CO_2 budgets was notable for North America and Southeast Asia. However, large gaps between the two methods remained in East Asia and South America. In other regions, Europe, boreal Asia, Africa, South Asia, and Oceania, it was difficult to determine whether those regions act as a net sink or source because of the large spread in estimates from atmospheric inversions. These results highlight two research directions to improve the robustness of CO_2 budgets: (1) to increase representation of processes in biosphere models that could contribute to fill the budget gaps, such as forest regrowth and forest degradation, and (2) to reduce sink-source compensation between regions (dipoles) in atmospheric inversion so that their estimates become more comparable. Advancements on both research areas will increase the level of agreement between the top-down and bottom-up approaches and yield more robust knowledge of regional CO_2 budgets.

Keywords: terrestrial CO_2 budget, net CO_2 flux, atmospheric inversion, biosphere model, carbon stock change, residual land uptake, land-use change emissions, riverine carbon export, CO_2 evasion

1. INTRODUCTION

Understanding the mitigation potential of the terrestrial biosphere against anthropogenic CO_2 emissions hinges upon accurate assessment of the net atmosphere-land CO_2 flux (net CO_2 flux, - for a net sink and + for a net source). Our ability to diagnose CO_2 sink-source patterns of the net CO_2 flux has progressed owing to the development of "top-down" atmospheric inversions (Peylin et al., 2013; Thompson et al., 2016) and "bottom-up" biosphere models (Sitch et al., 2008, 2015). Compared with early studies that varied by more than 3.0 Pg C yr^{-1} in their estimates of northern and tropical CO_2 fluxes (e.g., Gurney et al., 2002; Jacobson, Fletcher, Gruber, Sarmiento, & Gloor, 2007; Peylin, Baker, Sarmiento, Ciais, & Bousquet, 2002; Rödenbeck, Houweling, Gloor, & Heimann, 2003), net CO_2 fluxes by current atmospheric inversions are converging around a sink of 1.0 to 2.0 Pg C yr^{-1} in northern extratropical (NE) lands and a small net flux in southern−tropical (ST) lands, due to improvements in the transport processes modeling and abundance of aircraft and vessel observations, along with improved in situ CO_2 observation networks (Gaubert et al., 2019; Stephens et al., 2007). Likewise, net CO_2 fluxes simulated by biosphere models have become roughly consistent with this pattern, especially in ST lands, due to the offset of land-use change (LUC) emissions with enhanced CO_2 uptake by the stimulating effect of rising atmospheric CO_2 on plant photosynthesis (Schimel, Stephens, & Fisher, 2015). However, disagreements in the CO_2 budgets between top-down and bottom-up approaches remain nontrivial at regional scales (Cervarich et al., 2016; Ciais et al., 2013; Kondo, Ichii, Takagi, & Sasakawa, 2015). In the fifth assessment report of Intergovernmental Panel on Climate Change (IPCC AR5), the sign and magnitude of regional CO_2 budget estimates were still contradictory between atmospheric inversions and biosphere models for some regions (Ciais et al., 2013).

These previous syntheses highlight the challenges of reconciling the top-down and bottom-up approaches and the importance of spatial scale in evaluating agreement and uncertainties. When comparing CO_2 budgets of multiple methods, understanding the definition of the net CO_2 flux and associated component fluxes that are included in developing the CO_2 budgets become increasingly important because these could lead to either a "total" or "partial" exchange of CO_2 between the atmosphere and land depending upon the methods employed. The former applies to methods that use atmospheric CO_2 concentrations as a basis for estimation such as atmospheric inversions (Peylin et al., 2013). The latter applies to methods that account for known processes in the carbon cycle interacting with the biosphere such as biosphere models (Sitch et al., 2015). Major terms that cause challenges in comparing atmospheric inversions and biosphere models at the time of the IPCC AR5 can be: (1)

hydrosphere fluxes, such as lateral riverine carbon export and CO_2 evasion from rivers and lakes, included in atmospheric inversions, but not simulated in biosphere models, and (2) the incomplete representation of CO_2 fluxes from land-use and management in biosphere models. Mitigating these differences in terminology will advance our understanding of net CO_2 flux at regional scales which so far has remained unresolved.

To address the current state of our knowledge on terrestrial CO_2 budgets and the level of reconciliation between current modeling methods, CO_2 budget assessments at global, hemispheric, and regional scales need to be reanalyzed with consistent datasets and definitions of the component fluxes that determine net CO_2 flux. Based on the net CO_2 flux defined as "the atmosphere-biosphere CO_2 exchange" (excluding hydrosphere fluxes), we investigate net CO_2 fluxes estimated for the decade of 2000s (2000−2009) using fluxes adjusted around a consistent definition of the CO_2 exchange. These are compared with reproduced results of the IPCC AR5 obtained using inconsistent definitions, to determine how definitions play a role in reconciliation between the modeling methods. Aimed at serving as a useful reference, this study provides a thorough comparison between atmospheric inversions and biosphere models, and also among other existing estimates of global and regional CO_2 budgets based on forest inventories, remote sensing, atmospheric O_2 measurements, the residuals from non-terrestrial components of global CO_2 budgets, and previous regional budget assessments from the REgional Carbon Cycle Assessment and Processes (RECCAP, Canadell et al., 2011). Through these comparisons, we highlight potential difficulties faced by current CO_2 budget assessments, and suggests ways forward to increase the level of agreement between top-down and bottom-up approaches yielding more robust knowledge of CO_2 budgets.

2. MATERIALS AND METHODS

2.1 Definition of net CO_2 flux

We define the net CO_2 flux as the "atmosphere-biosphere CO_2 exchange", comprising components such as photosynthesis, autotrophic and heterotrophic respirations, fire emissions, and CO_2 fluxes associated with land-use and land-cover changes. Adjustments based on the proposed definition of net CO_2 flux were applied to the methods described herein where relevant (Fig. 1; Spatial and temporal applicability of the methods is shown in Table S1). Biosphere models comply with this definition, as they consider numerous processes of atmosphere-land biogeochemistry, including LUC fluxes in the latest development (Le Quéré et al. 2018a). A method based on carbon stock changes from the

compilation of forest inventories (ΔC_{IM}, Pan et al., 2011) also complies with this definition. The Vegetation Optical Depth (VOD) derived from passive microwave sensors (e.g., Liu et al., 2015) is only applicable to aboveground vegetation, but can be supplemented by inventories of missing belowground components to represent the total stock change (ΔC_{VOD}). Methods that consider interactions beyond those with the biosphere, such as atmospheric inversions, and global land uptake assessments based on a residual of non-terrestrial components of global CO_2 budgets (residual method, Le Quéré et al., 2018a) and based on decadal O_2 and CO_2 trends in the atmosphere (O_2-based method, Keeling & Manning, 2014) can roughly comply with the proposed definition when the hydrosphere fluxes are excluded from their budget estimates, as we discuss further in this paper.

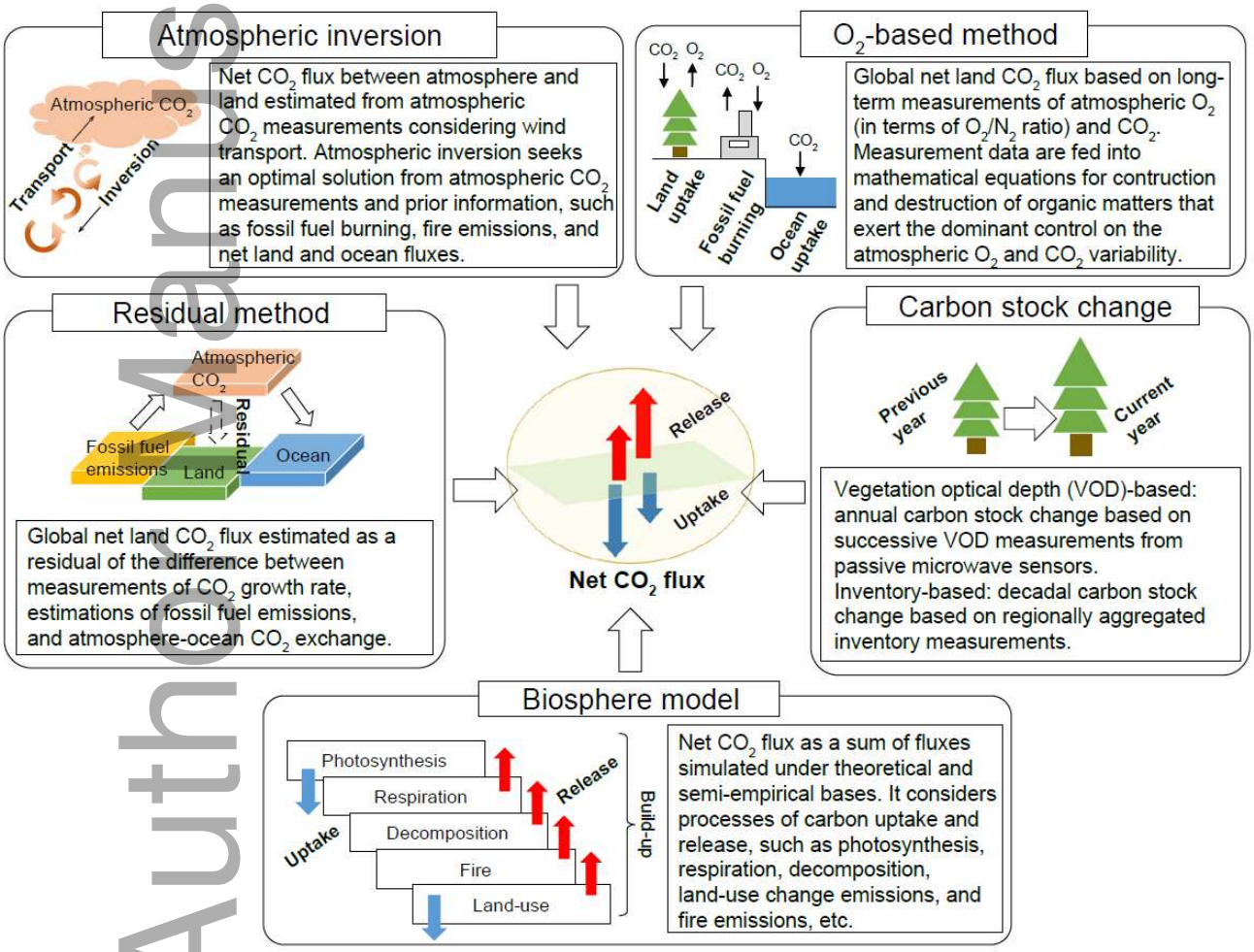

FIGURE 1. Methods of terrestrial net CO_2 flux estimation.

2.2 Independent methods of estimating net CO_2 flux

2.2.1 Atmospheric inversions

The net CO_2 flux from atmospheric inversions was represented by eight inversions (Table 1). These inversions estimate net CO_2 flux through the assimilation of continuous or discrete atmospheric CO_2 measurements from global networks (e.g., World Data Centre for Greenhouse Gases, WDCGG; and the observation package (ObsPack) from the NOAA Earth System Research Laboratory, NOAA/ESRL) in transport model, with prior information (e.g., net land flux, net ocean flux, fire emissions, and fossil fuel emissions). The choices of CO_2 measurements and prior fluxes differ for each inversion system, as well as the spatial resolution and period of inverted fluxes (Table 1).

For each inversion, posterior land flux was adjusted by the difference between the respective fossil fuel emissions prescribed in the inversion and a reference emission estimate. This "fossil fuel adjustment" is a necessary procedure for reducing variability in posterior fluxes, as differences in prescribed fossil fuel emissions largely affect posterior fluxes (Peylin et al., 2013), especially for recent periods for which the uncertainty in fossil fuel emissions remains large (Ballantyne et al., 2015). We applied the fossil fuel adjustment using the emission dataset prescribed in ACTM (Table 1), showing a central tendency of global interannual variability among inversions, as the reference emission.

189 **TABLE 1.** Configuration of the atmospheric CO_2 inversion systems used in this study.

Inversion system (in-text abbreviation)	No. of region	Time period	IAV prior[#]	No. of observations	Transport model	Meteorology	Prior fluxes				Reference
							Land	Ocean	Biomass Burning	Fossil fuel emissions	
ACTM (ACTM)	84	1990–2011	Yes: FF, LA No: SA	73 (GLOBALVIEW)	JAMSTEC's Atmospheric Chemistry-Transport Model (ACTM)	NCEP	Three-hourly flux from CASA	Monthly flux from the LDEO (Takahashi) Surface pCO_2 database	--	EDGAR v4.2 rescaled global total to CDIAC	Saeki & Patra (2017)
MIROC4-ACTM (MACTM)	84	1996–2015	Yes: FF, LA No: SA	42 sites (NOAA ESRL ObsPack & JMA)	Updated ACTM with MIROC4-ESM	JRA-55	Three-hourly flux from CASA	Monthly flux from the LDEO	--	EDGAR v4.3.2	Patra et al. (2018); Le Quéré et al. (2018b)
CAMS v18r1 (CAMS)	Grid cells (3.75˚ × 2.5˚)	1979-2015	Yes: FF No: BB, LA, SA	81 (NOAA ESRL ObsPack)	Tracer Transport Model version 5 (TM5)	ECMWF	Three-hourly flux from ORCHIDEE	Monthly flux from the LDEO (Takahashi) Surface pCO_2 database	GFAS	EDGAR v4.2 rescaled global total to CDIAC	Chevallier et al. (2010)
CCAM (CCAM)	94 land, 52 ocean	1993-2012	Yes: FF No: LA, SA	69 (GLOBALVIEW)	CSIRO Conformal-cubic Atmospheric Model (CCAM)	NCEP	Monthly flux from CASA	Monthly flux from the LDEO (Takahashi) Surface pCO_2 database	--	EDGAR v4.2 rescaled regionally to CDIAC	McGregor & Dix (2008)
Carbon Tracker2017 (CT2017)	Grid cells (1.0˚ × 1.0˚)	2000-2016	Yes: FF, BB, LA, SA	254 (from 55 institutions)	Tracer Transport Model version 5 (TM5)	ECMWF and ERA	Monthly CASA flux downscaled to 90-minute flux	Ocean inversion fluxes and monthly flux from the LDEO Surface pCO_2 database	GFED4.1s and GFED_CMS	ODIAC2016 and Miller emissions datasets	Peters et al. (2007)
GELCA_CAO (GELCA CAO)	Grid cells (1.0˚ × 1.0˚)	2000-2013	Yes: FF, BB. LA, SA	NOAA ESRL ObsPack	Coupled GELCA-NIES 08.1 Eulerian model	JCDAS	Daily flux from VISIT	Monthly flux from 4D-var + OTTM based on	GFED	ODIAC	Zhuravlev, Khattatov, Kiryushov, &

								pCO_2 data			Maksyutov (2011)
JENA s93_v4.2 (JENA s93)	Grid-cells (about 4.0˚ × 5.0˚)	1993-2016	Yes: FF No: LA, SA	35 (from various institutions)	Tracer Transport Model version 3 (TM3)	NCEP	Zero values	Monthly climatological flux based on an interpolation of pCO_2 data	--	Monthly values from CDIAC	Rödenbeck, Zaehle, Keeling, & Heimann (2018)
JMA2018 (JMA)	22	1985–2016	Yes: FF, SA No: LA	88 (WDCGG) 16 (aircraft observations), 59 (vessel observations)	JMA atmospheric transport model (based upon JMA global weather forecasting model)	JRA-55	Monthly flux from CASA	Monthly flux from the JMA (Iida et al., 2015)	--	CDIAC2016 rescaled global total to Global Carbon Budget (2017v1.2)	Update of Maki et al. (2010)

#Abbreviations: biomass burning emission (BB), fossil fuel emission (FF), land-air CO_2 exchange (LA), and sea-air CO_2 exchange (SA).

2.2.2 Biosphere models

Simulations from TRENDY v6 (Le Quéré et al., 2018a) represent the net CO_2 flux from the biosphere models of this study (Table 2). These simulations were prepared with a consistent forcing dataset: a global atmospheric CO_2 concentrations for 1860−2016 based on ice core measurements and stationary observations from NOAA, a gridded climate dataset (CRU-NCEP v8) for 1901−2016 (Viovy, 2018), and a gridded annual land-use and land-cover change dataset for 1860−2016 (Hurtt et al., 2017; Klein Goldewijk, Beusen, Doelman, & Stehfest, 2017). The TRENDY models carried out three types of simulations: S1 that used varied atmospheric CO_2, fixed climate (1901−1920) and fixed land-use and land-cover (1860), S2 that used varied CO_2 and climate (with fixed land-use and land-cover at 1860), and S3 that varied all three drivers. For each simulation, the models first established an equilibrium carbon balance by a spin-up run, forced with the 1860 CO_2 concentration (287.14 ppm), recycling climate variability from 1901−1920, and constant 1860 crop and pasture distributions.

Attributes of the net CO_2 flux (i.e. the effects of CO_2, climate, and LUC) were extracted by separating flux signals in the S1, S2, and S3 simulations (Friedlingstein et al., 2006). The net CO_2 flux of S3 represented the estimate most closely matching observations, including the interactions between CO_2, climate, and LUC effects on the ecosystem carbon cycling. Those from S1 and S2 represented partial contributions to the net CO_2 flux, isolating the CO_2 effect and CO_2+climate effects on the net CO_2 flux, respectively. The LUC effect on the net CO_2 flux was extracted by subtracting estimates of S2 from that of S3. Similarly, the effect of climate was extracted by subtracting the net CO_2 flux of S1 from that of S2.

212 **TABLE 2.** Configuration of the TRENDY models used in this study.

Biosphere model	Spatial resolution	Carbon-Nitrogen coupling	Fire simulation (including peat fire)	Age class	Land use change scheme					Reference
					Distinction between primary and secondary lands	Wood harvest	Shifting cultivation	Crop harvest (crop species: C, managed grassland :G)	Degradation	
CABLE	0.5˚ × 0.5˚	Yes	No	Yes	Yes	Yes	Yes	Yes: G	No	Haverd et al. (2018)
CLM	1.9˚ × 2.5˚	Yes	Yes (Yes)	No	Yes	Yes	Yes	Yes: G	No	Oleson et al. (2013)
DLEM	0.5˚ × 0.5	Yes	No	No	Yes	Yes	No	Yes: G	No	Tian et al. (2015)
ISAM	0.5˚ × 0.5˚	Yes	No	No	Yes	Yes	No	Yes: G	No	Jain, Meiyappan, Song, & House (2013)
LPJ-GUESS	0.5˚ × 0.5˚	Yes	Yes (No)	No	Yes	Yes	Yes	Yes: C	No	Smith et al. (2014)
LPJ-wsl	0.5˚ × 0.5˚	No	Yes (No)	No	Yes	No	No	Yes: G	No	Sitch et al. (2003)
LPX-Bern	1.0˚ × 1.0˚	Yes	Yes (No)	No	No	No	No	Yes: G	No	Keller et al. (2017)
ORCHIDEE	0.5˚ × 0.5˚	No	No	No	Yes	Yes	No	Yes: G	No	Krinner et al. (2005)
ORCHIDEE-MICT	1.0˚ × 1.0˚	No	Yes (No)	No	Yes	No	No	Yes: C	No	Guimberteau et al. (2018)
VISIT	0.5˚ × 0.5˚	No	Yes (No)	No	Yes	Yes	Yes	Yes: G	No	Kato, Kinoshita, Ito, Kawamiya, & Yamagata (2013)

2.2.3 Carbon stock changes, O_2-based method, residual method, and RECCAP

Inventory-based carbon stock changes (ΔC_{IM}) were estimated by incorporating information on forest area and biomass density obtained from (i) United Nations Global Forest Resources Assessment reports (Food and Agriculture Organization, 2006, 2010), (ii) deforestation and afforestation estimates from a book-keeping model (Houghton, 2007), and (iii) the observed carbon pools for regions around the globe. From these datasets, the sums of carbon stocks for intact and regrowth forests and soil carbon for 2000 and 2007 were used to calculate regional carbon stock changes (Pan et al., 2011), except for South Asia where a missing estimate was supplemented by inventory and forest area data for 1992−2002 from Kaula, Dadhwal, and Mohren (2009). To estimate VOD-based carbon stock change (ΔC_{VOD}) for the 2000s, we used the satellite-derived gridded aboveground biomass from Global Aboveground Biomass Carbon v1.0 (Liu et al., 2015). The VOD-based aboveground biomass is estimated based on an empirical relationship between the gridded aboveground biomass for tropical regions (Saatchi et al., 2011) and harmonized passive microwave observations. VOD only measures aboveground backscatter, therefore belowground biomass was estimated as a constant fraction of the estimated aboveground biomass (Liu et al., 2015). To provide more reliable estimates, we replaced this belowground biomass of ΔC_{VOD} with the data used for ΔC_{IM}.

The O_2-based method provides a mean annual global CO_2 budget for the land and ocean based on destructive and constructive O_2 and CO_2 processes (Keeling & Manning, 2014). This approach utilizes long-term measurements of CO_2 and the O_2/N_2 molar ratio between a sample and a reference, expressed as $\delta(O_2/N_2)$, as changes in the global mean molar fraction of CO_2 and $\delta(O_2/N_2)$ are related to the net sources and sinks of CO_2, O_2, and N_2 in the atmosphere. The budget used in this study was estimated for 2000–2010 by Keeling and Manning (2014). The residual method from the Global Carbon Project (Le Quéré et al., 2018a) provided the global annual budget of land CO_2 uptake calculated as the difference between the other terms in the global carbon budget, i.e., fossil fuel emissions minus the CO_2 growth rate and the net ocean uptake simulated by biogeochemical models. The budget of this method for the 2000s was calculated using the data of Le Quéré et al. (2018a). The RECCAP project quantified regional anthropogenic and biogenic CO_2 budgets by integrating CO_2 fluxes from multiple independent approaches, including biosphere models, atmospheric inversions, and inventories (Canadell et al., 2011). Based on the available major and minor fluxes and through consideration of the reliability of each of the

fluxes, the regional CO_2 budget was estimated for global regions. The regional budgets used in this study were from re-calculated estimates based on the RECCAP studies in Li et al. (2016).

2.3 Adjustments for the atmosphere-biosphere CO_2 exchange estimation

To yield the atmosphere-biosphere CO_2 exchange, global gridded data of lateral riverine carbon export and CO_2 evasion from rivers and lakes were used to remove the hydrosphere components from the fossil fuel adjusted CO_2 budgets of the atmospheric inversions. Global lateral riverine carbon including dissolved organic and inorganic carbon (DOC and DIC, respectively) was obtained from the multi-form model of nutrient exports by NEWS 2 (Mayorga et al. 2010). Global river CO_2 evasion was derived from the empirical river water pCO_2 model and global maps of stream surface area and gas exchange velocities (Lauerwald, Laruelle, Hartmann, Ciais, & Regnier, 2015). Global lake CO_2 evasion was estimated based on lake pCO_2, total lake/reservoir surface area, and total CO_2 evasions for 231 coastal regions (Raymond et al., 2013), subsequently downscaled to a continuous grid scale via the Global Lakes and Wetland Database (Zscheischler et al., 2017).

These data were also used to derive the atmosphere-biosphere CO_2 exchange for the O_2-based method and RECCAP. The O_2-based method and RECCAP account for lateral riverine exports as a part of the land biosphere flux. Thus, we excluded annual riverine DOC and DIC fluxes from the global budget estimates of both methods using the data described above. Global CO_2 uptake by the residual method includes only riverine carbon exports due to anthropogenic perturbations (Le Quéré et al., 2018b). To remove that flux from the residual method, an estimate of the anthropogenic component of river flux from Regnier et al. (2018) was used.

2.4 A constraint for the global budget

Owing to atmospheric observations, the CO_2 budget at the global scale is the best understood among those at other scales (Le Quéré et al., 2018a). To analyze CO_2 budgets at multiple scales, it is important to have consistent global CO_2 budgets so that results of hemispheric and regional budgets would not be misinterpreted due to outliers of global budget estimates. Therefore, we defined a criterion, based on the global CO_2 budget from the residual method and ±1.0 Pg C yr^{-1} uncertainties, to constrain global CO_2 budgets from the top-down and bottom-up models for the 2000s. All eight atmospheric inversions of this study satisfied this criterion, since the atmospheric CO_2 growth rate was used to constraint atmospheric

inversions. As for biosphere models, among the TRENDY models that provided net CO_2 fluxes of all three experiments, ten models satisfied this criterion (Table 2).

3. GLOBAL AND HEMISPHERIC BUDGETS

To articulate differences from results of the IPCC AR5, we compared experiments from TRENDY (S2: not including time-varying LUC simulation, and S3: including time-varying LUC simulation), and atmospheric inversions before (INV) and after correcting for the hydrosphere components (INV_{AB} denotes inversions adjusted for the atmosphere-biosphere CO_2 exchange). TRENDY S3 and INV_{AB} represented "best estimates" of the net CO_2 flux, and TRENDY S2 and INV represented estimates reproduced using the IPCC AR5 configuration (Fig. 2). As illustrated in Figure 3a, global CO_2 budgets by TRENDY S2 (-2.6 [-2.9, -2.1] Pg C yr^{-1}: medians [lower, upper quartiles]) and INV (-2.3 [-2.5, -1.7] Pg C yr^{-1}) largely overestimated the amount of CO_2 uptake compared with other independent estimates: ΔC_{VOD} (-1.2 Pg C yr^{-1}), ΔC_{IM} (-1.2 Pg C yr^{-1}), the residual method (-0.9 Pg C yr^{-1}), O_2-based method (-0.7 Pg C yr^{-1}), and RECCAP (-1.3±0.6 Pg C yr^{-1}, mean±1σ). This overestimated CO_2 uptake is likely a consequence of missing and excess components needed to satisfy the net CO_2 flux definition. Meanwhile, upward shifts in the net CO_2 flux caused by accounting for LUC emissions in the biosphere models and discounting the hydrosphere fluxes in the atmospheric inversions led to a close agreement in global CO_2 budgets with respect to the other independent estimates and with each other, where TRENDY S3 estimated -0.9 [-1.4, -0.8] Pg C yr^{-1} and INV_{AB} estimated -0.9 [-1.2, -0.4] Pg C yr^{-1} (Fig. 3a; interannual variability (IAV) shown in Fig. S1).

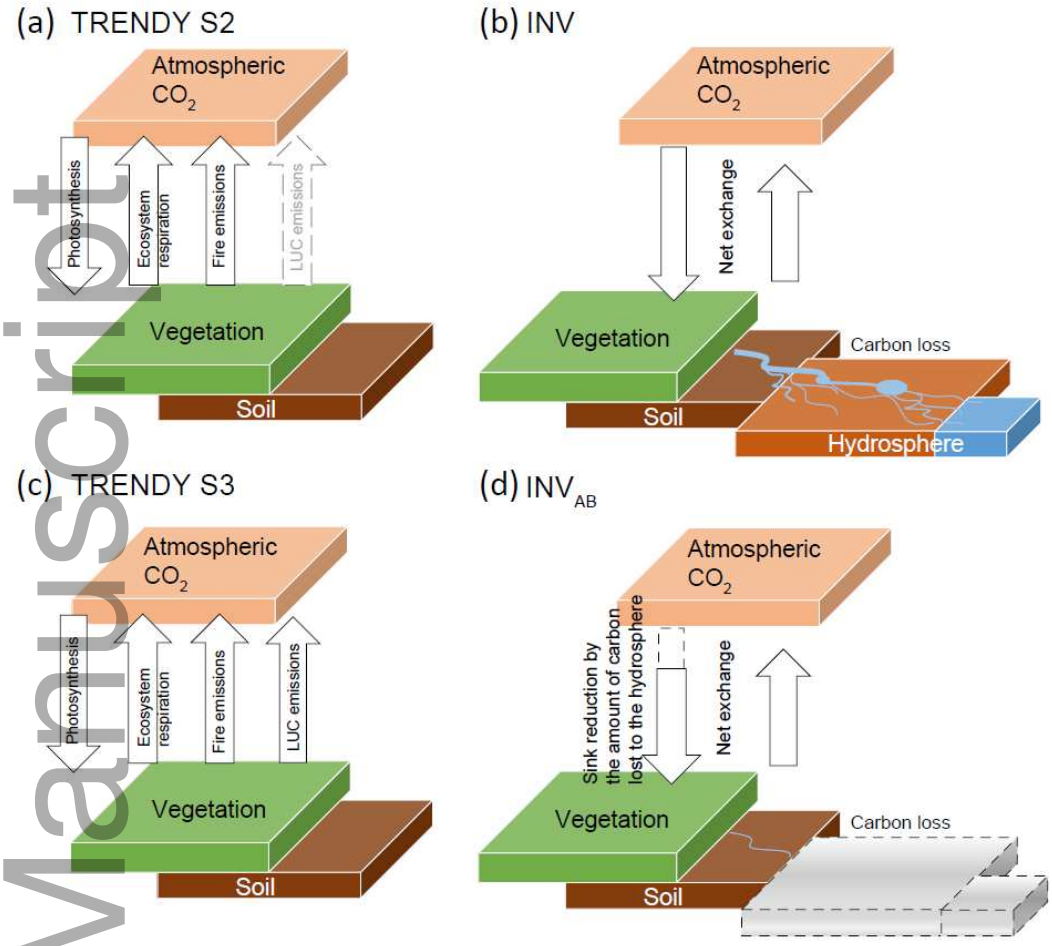

FIGURE 2. Differences in definition of the net CO_2 flux. Schematics show the components of the net CO_2 flux considered in: **a)** TRENDY S2 (biosphere models without LUC), **b)** INV (atmospheric inversions including hydrospheric components), **c)** TRENDY S3 (biosphere models including LUC), and **d)** INV_{AB} (atmospheric inversions excluding hydrospheric components).

The global CO_2 budget largely consists of fluxes from northern boreal-temperate and pantropical ecosystems, with the former accounting for a large part of the global sink and the latter for a large part of the global LUC emissions (Ciais et al., 2019; Le Quéré et al., 2018b). That is, the well-constrained global CO_2 budgets among the methods should accompany a consistent budget partitioning between those regions. To evaluate this aspect, we applied the so-called "diver down" plot of Schimel, Stephens, and Fisher (2015) to better understand global CO_2 budget partitioning into NE and ST lands (Fig. 3b, c). The reproduced IPCC AR5 results (TRENDY S2 and INV) exhibited limited overlap with each other (Fig. 3b). INV produced relatively strong sinks of -1.2 to -2.5 Pg C yr^{-1} in NE and a small net flux in ST

lands. With the absence of LUC emissions, TRENDY S2 resulted in a net sink for both NE and ST lands, spanning approximately -1.0 to -2.0 Pg C yr^{-1}. Including simulated LUC fluxes in biosphere models and removing the hydrosphere fluxes from atmospheric inversions shifted the NE and ST land fluxes of the two methods towards a reduced sink or net source, leading to an overlap between TRENDY S3 and INV_{AB} (Fig. 3c; IAV shown in Fig. S2) and with ΔC_{VOD}, ΔC_{IM}, and RECCAP (Fig. 3c). However, agreements between TRENDY S3 and INV_{AB} are not yet robust, as the distribution of INV_{AB} leans more towards a net sink in NE lands (-2.2 to -0.7 Pg C yr^{-1}) and a net source in ST lands (-0.4 to 1.0 Pg C yr^{-1}) than that of TRENDY S3: -2.0 to -0.5 Pg C yr^{-1} in NE and -1.1 to 0.6 Pg C yr^{-1} in ST lands.

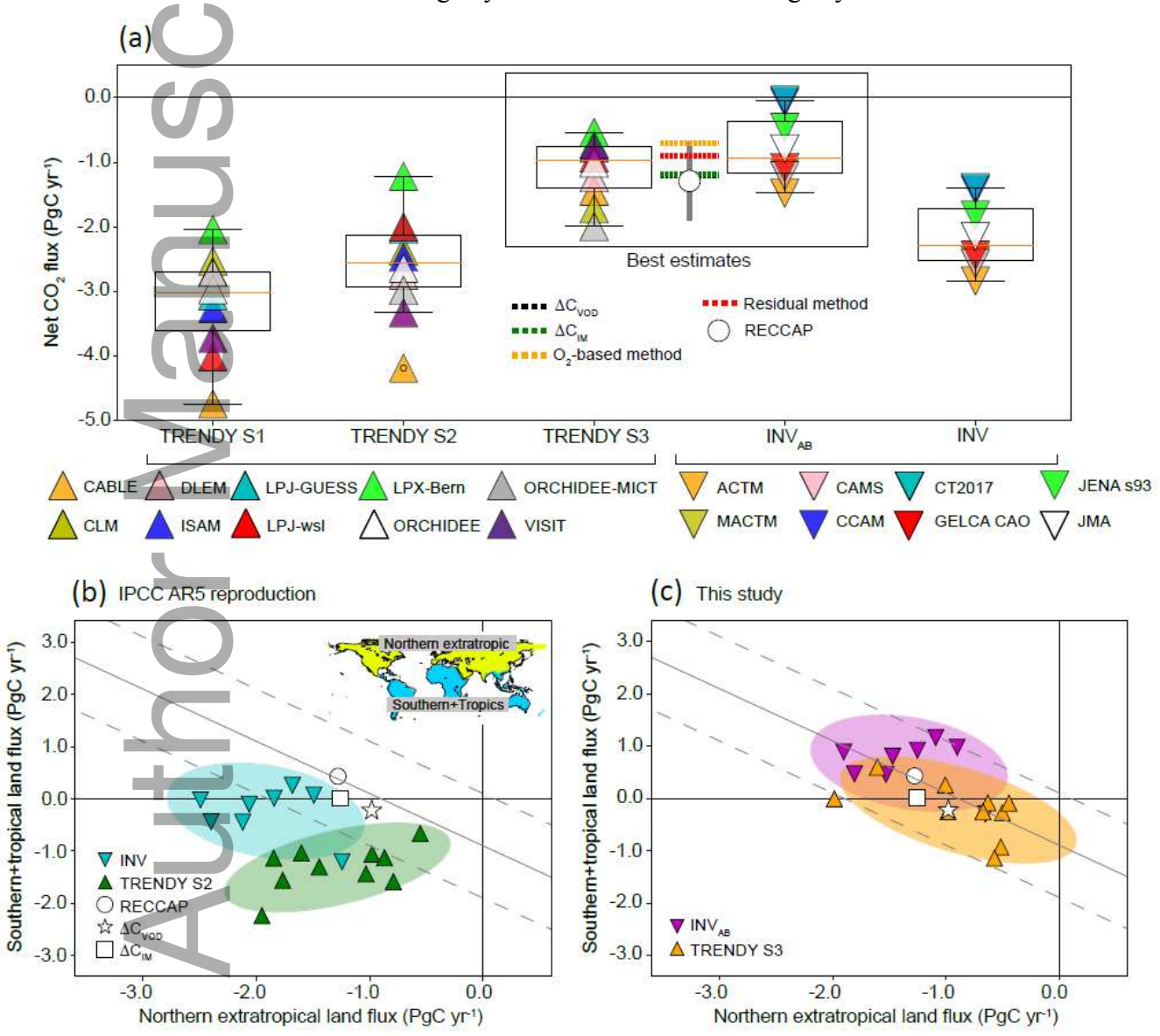

FIGURE 3. Improved agreement of global and hemispheric net CO_2 flux estimates over the IPCC AR5. **a)** Global CO_2 budgets for the 2000s from the biosphere models (upper triangles), atmospheric inversions (lower triangles),

carbon stock changes: ΔC_{VOD} (black dashed line) and ΔC_{IM} (green dashed line), O_2-based method (yellow dashed line), residual method (red dashed line), and estimates from the RECCAP project (circle representing the mean value and bar representing the 1σ uncertainty). Box plots are shown for the biosphere models (three TRENDY simulations, S1, S2, and S3) and atmospheric inversions (INV and INV_{AB}). Partitioning of the global CO_2 budget into northern extratropical (NE) and southern-tropical (ST) lands (diver-down plot) for **b)** TRENDY S2 and INV (IPCC AR5 reproduction), and **c)** TRENDY S3 and INV_{AB} (results from this study). Gray lines are the constraint on global CO_2 budgets represented by the global budget estimate from the residual method, with ±1.0 Pg C yr^{-1} uncertainty. Results that fall within the constraints are combinations of NE and ST land budgets that preserve the reference value of global CO_2 budget. Individual model estimates and error ellipse of 2σ range are shown for TRENDY S2 and S3 (green and orange upper triangles, respectively), and INV and INV_{AB} (cyan and purple lower triangles, respectively), along with the independent estimates from carbon stock changes: ΔC_{VOD} and ΔC_{IM} (star and square, respectively) and estimate from the RECCAP project (circle representing the mean value).

Figure 3c illustrates the results only of the net balance of CO_2 fluxes. To gain confidence in the overlapping pattern between the two methods, it is necessary to understand changes in the patterns of sinks and sources induced by the major processes governing the net CO_2 flux. The effect of increasing CO_2 concentration on photosynthesis (the CO_2 effect) is considered the dominant driver of current terrestrial CO_2 uptake (Keenan et al., 2016; Keenan & Williams, 2018; Kondo et al., 2018a; Schimel, Stephens, & Fisher, 2015), and LUC activities (the LUC effect) are the major net emissions source from ecosystems to the atmosphere (Arneth et al., 2017; Kondo et al., 2018b). The net CO_2 flux of TRENDY S3 decomposed into three attributes confirms that the CO_2 and LUC effects are the major sink and source components in NE and ST lands, respectively (Fig. 4a). However, the climate effect should not be overlooked, as it induces substantial changes in sink-source patterns during El Niño and La Niña phases, especially in ST lands (Fig. 4a). Importantly, the overlap between TRENDY S3 and INV_{AB} holds not only for the decadal mean (Fig. 3c), but also for the El Niño and La Niña phases during the 2000s (Fig. 4b; IAV and seasonality of ST land fluxes shown in Fig. S3), indicating that large-scale flux changes in response to El Niño-Southern Oscillation (ENSO) are similar in the atmospheric inversions and biosphere models.

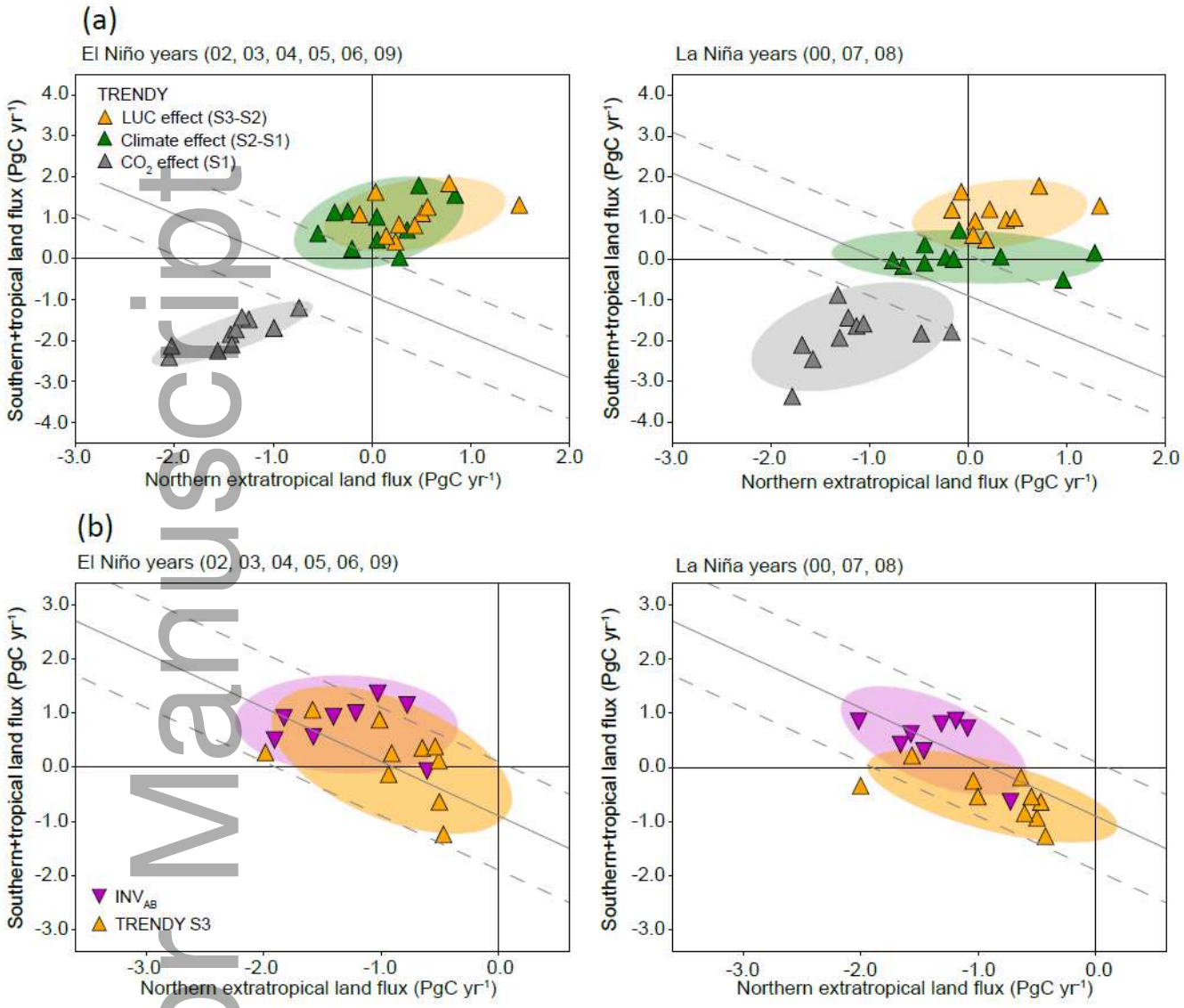

FIGURE 4. Patterns of global CO_2 budget partitioned into hemispheres under ENSO variability. Partitioning of global CO_2 budget into NE and ST lands (diver-down plots), during El Niño years (2002, 03, 04, 05, 06, and 09) and La Niña years (2000, 07, and 08) are shown for: **a)** each attribute of the net CO_2 flux by TRENDY S3, CO_2 effect (TRENDY S1: grey upper triangles), climate effect (TRENDY S2-S1: green upper triangles), and LUC effect (TRENDY S3-S2: orange upper triangles) and **b)** the net CO_2 fluxes of INV_{AB} and TRENDY S3. El Niño years are the years that have six-month averaged Multivariate ENSO Index (MEI) values >0.5 within a year, and La Niña years are the years that have MEI values <-0.5 within a year. Gray lines represent the global budget constraint and ±1.0 Pg C yr^{-1} uncertainty same as in Figure 3c.

4. REGIONAL BUDGETS

We further partitioned hemispheric budgets into nine regions. Regional CO_2 budgets were overall comparable between TRENDY S3 and INV_{AB}, but the degree of agreement differed by region (Fig. 5; IAV shown in Fig. S4). Among the nine regions, the ranges of budget estimates were proximate among INV_{AB}, TRENDY S3, and the other independent estimates for North America and Southeast Asia. A notable improvement was identified in Southeast Asia, where reduced CO_2 sinks by accounting for LUC fluxes in biosphere models and discounting for the hydrosphere fluxes from atmospheric inversions resulted in close agreement between INV_{AB} (0.01 [-0.04, 0.20] Pg C yr^{-1}) and TRENDY S3 (-0.01 [-0.06, 0.10] Pg C yr^{-1}). Budget estimates for Europe, boreal Asia, Africa, South Asia, and Oceania overlapped, but with a larger range in INV_{AB} than in TRENDY S3 (Fig. 5). In Africa, adjustments for the missing and excess fluxes in the two modeling methods seemingly mitigated the gap between median INV and TRENDY S2 values; however, a range > 1.0 Pg C yr^{-1} in the individual estimates of INV_{AB} rendered comparison with TRENDY S3 difficult.

Budget estimates for East Asia and South America showed notable differences between INV_{AB} and TRENDY S3 (Fig. 5). In East Asia, the budget estimates by both INV_{AB} and TRENDY S3 indicated a net sink, but INV_{AB} (-0.5 [-0.7, -0.3] Pg C yr^{-1}) leaned towards a greater net sink than TRENDY S3 (-0.07 [-0.20, -0.01] Pg C yr^{-1}). In South America, INV_{AB} leaned towards a net source contrary to the net sink indicated by TRENDY S3. The gap in South America was the most notable, with budget estimates barely overlapping between INV_{AB} (0.6 [0.5, 0.8] Pg C yr^{-1}) and TRENDY S3 (-0.2 [-0.3, -0.1] Pg C yr^{-1}). In this region, the flux adjustments did not reduce the gap in budgets. Importantly, these differences explained the minor deviation in the distributions of global budget partitioning into hemispheres between INV_{AB} and TRENDY S3 (Fig. 3c). The differences between budget estimates for East Asia are largely responsible for INV_{AB} indicating a stronger net sink in NE lands than TRENDY S3. Likewise, the differences in the estimates for South America are responsible for the INV_{AB} indicating a stronger net source in ST lands than those of TRENDY S3. Thus, East Asia and South America are the regions where future model improvements are needed to generate CO_2 budgets that agree at the hemispheric and regional scales.

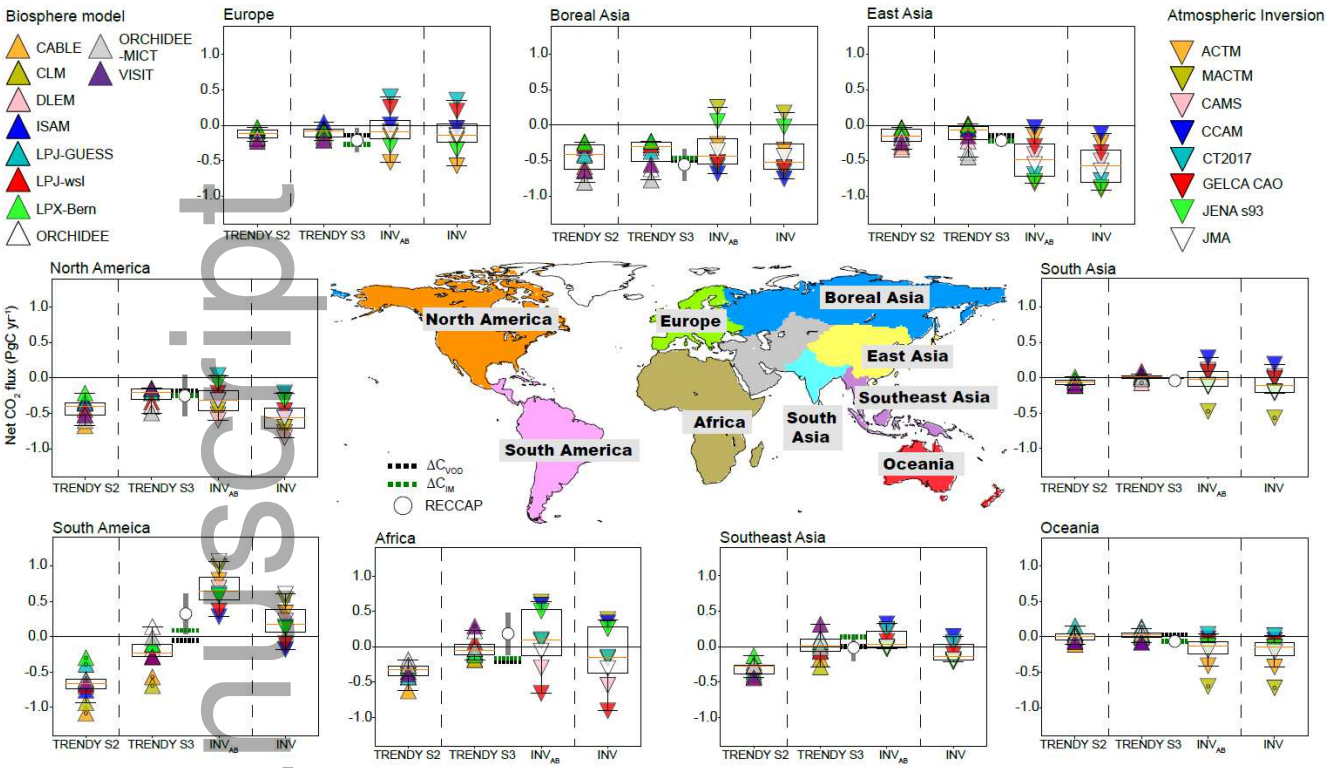

FIGURE 5. Consistency and inconsistency among the estimates of regional CO_2 budgets. Regional CO_2 budgets for the 2000s by the biosphere models (TRENDY S2 and S3) and atmospheric inversions (INV and INV_{AB}), carbon stock changes (ΔC_{VOD} and ΔC_{IM}), and RECCAP project. Regional classification is based on the RECCAP studies. Colors and symbols are the same as in Figure 3a.

So far, we evaluated the regional CO_2 budgets in terms of the average patterns of the atmospheric inversions and biosphere models. However, to derive robust budget agreements for all regions, the means by which individual models partitioned hemispheric budgets into the nine regions must be further investigated. Contrary to the consistent pattern found in the global budget partitioning, individual INV_{AB} results showed largely different patterns for the partitioning of NE and ST land budgets (Fig. 6a). Some inversions showed a greater net source or reduced sink in Europe, corresponding to a greater net sink in boreal Asia, while others showed the opposite pattern between these two regions. This sink-source compensation was also identified between boreal Asia and East Asia, East Asia and South Asia, and South America and Africa, with large variabilities in their patterns. These results suggest that differences in the sink-source compensation are likely the major factor responsible for the large range found in regional budget estimates by INV_{AB} (Fig. 5). Although the magnitudes of budgets differed, the pattern of NE and ST land budget partitioning was overall similar among the models of TRENDY S3 (Fig. 6b).

Additionally, ΔC_{VOD}, ΔC_{IM}, and RECCAP showed close agreements in their patterns of partitioning (Fig. 6c), more closely resembling the average pattern of TRENDY S3 than that of INV_{AB}.

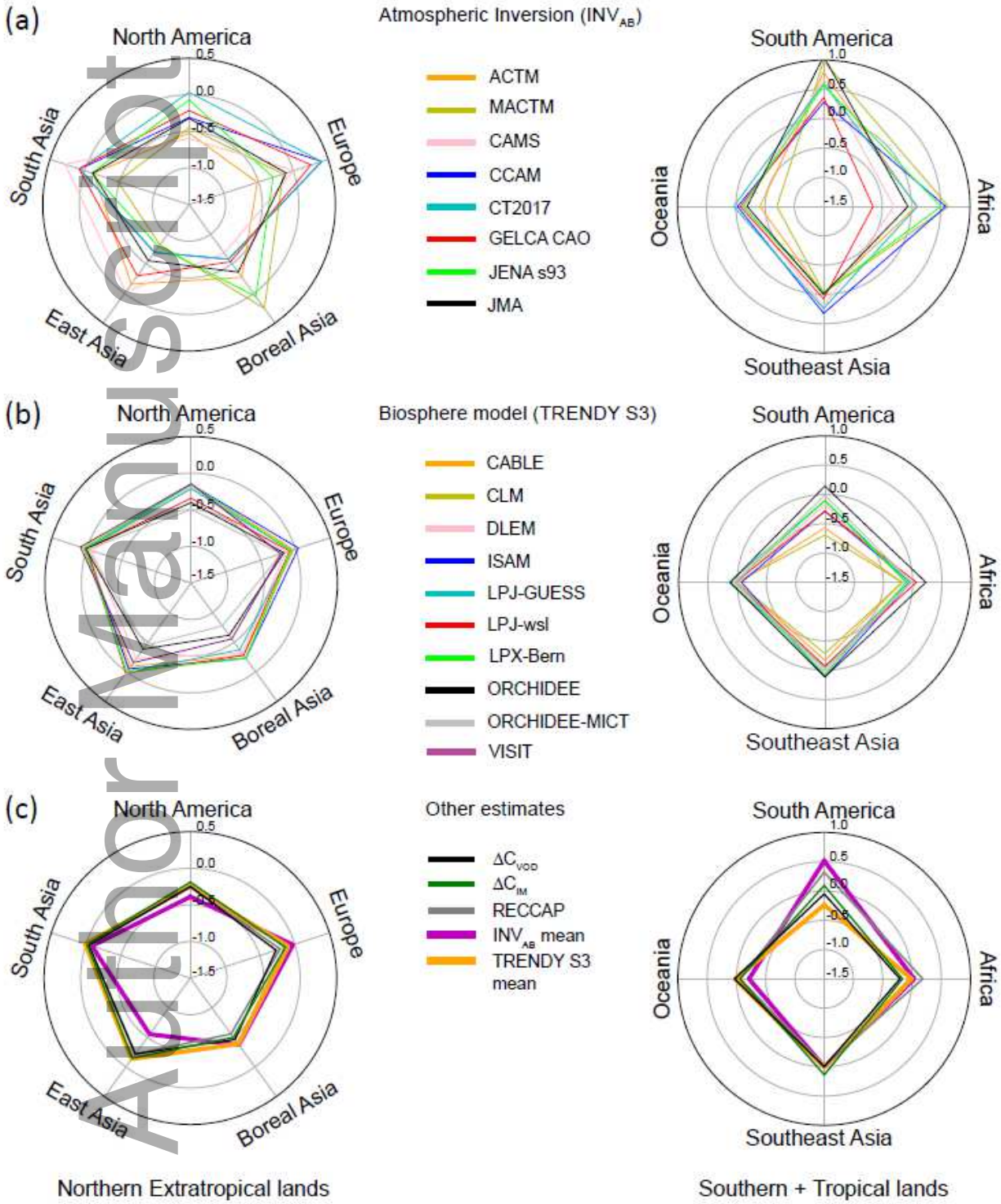

FIGURE 6. Multi-method comparison of hemispheric budget partitioning into regions. Partitioning of hemispheric budgets into corresponding regions by **a)** INV_{AB}, **b)** TRENDY S3, and **c)** means of INV_{AB} and

TRENDY S3, and other independent estimates (ΔC_{IM}, ΔC_{VOD}, and RECCAP). Partitioning of the NE land budget into five regions and the ST land budget into four regions are shown for each method. All figures are in units of Pg C yr^{-1}.

5. CHALLENGES FOR ESTIMATING REGIONAL CO_2 BUDGETS

Schimel, Stephens, and Fisher (2015) demonstrated a rough agreement in the global budget partitioning between atmospheric inversions that are capable of reproducing the observed annual vertical gradients of atmospheric CO_2 and biosphere models that simulate offsets between the CO_2 and LUC effects. The results of our study revealed that agreements between the latest atmospheric inversions and biosphere models are more consistent under a unified definition of the net CO_2 flux (Fig. 3c), confirming the roles of NE and ST lands in the global carbon cycle (Gaubert et al., 2019; Schimel, Stephens, & Fisher, 2015; Stephens et al., 2007). However, our results also emphasize that this level of agreement is insufficient to fully reconcile regional CO_2 budgets, as illustrated in Figure 5. In addition, a meta-analysis of individual estimates from TRENDY S3 and INV_{AB} indicates that the agreement between individual models found for particular regions does not necessarily hold true for the other regions (Fig. S5). This implies that we do not yet have an optimal combination of atmospheric inversions and biosphere models that is capable of producing consistent budget estimates for all global regions. To achieve consistent global, hemispheric, and regional CO_2 budgets between the two methods, we need to acknowledge some fundamental issues in modeling that should be resolved in future studies.

To produce regional CO_2 budgets with lower uncertainties, differences in the sink-source compensation ("the dipole effect"; Peylin, Baker, Sarmiento, Ciais, & Bousquet, 2002) among individual inversions need to be reduced. The dipole effect is intrinsic to the design of inversion systems, where the CO_2 budgets of neighboring regions connected via wind paths are tightly anti-correlated, because the sum of the regions is better constrained from the large-scale atmospheric signals than the individual regions. Europe and boreal Asia are a good example of this effect, with both exhibiting large variability, but a reverse order in the net sinks and sources of individual inversions (Fig. 6). While additional CO_2 observations could provide better constraints of the inversion system at global regions, this alone is unlikely to resolve the large variability among inversions. As notable variability was found in Europe, one of the regions characterized by a high density of in-situ CO_2 observations, we need to acknowledge a possibility that modeling issues are responsible for this variability. They include differences in prior datasets, model resolution, control vector size (a set of posterior CO_2 fluxes to be

estimated at given temporal and spatial resolutions), assimilation window length (the period during which data assimilation is conducted), transport rates (rates at which CO_2 is transported from a source region to neighboring regions through model atmosphere), and transport model errors (in particular concerning vertical mixing) among inversions. For example, the degree to which a regional budget reflects localized fossil fuel signals or CO_2 measurement signals varies with the resolution of the transport models and the size of the inversion control vector. These differences might have caused the large variability in the European CO_2 budgets, which then propagated into the budget estimates for boreal Asia via the dipole effect. Recent studies highlighted uncertainties in inter-hemispheric CO_2 transports as one of the causes behind the variability in zonal CO_2 budgets among inversions (Le Quéré et al., 2018b; Schuh et al., 2019). The variability co-occurring between neighboring regions indicates a possibility that a non-negligible level of uncertainties may exist in intra-hemispheric transports as well.

Contrary to atmospheric inversions, the biosphere models produced a relatively consistent pattern of hemispheric budget partitioning (Fig. 6b), however, this does not mean that the results are more reliable. Biosphere models still poorly represent certain processes, such as forest regrowth, cropland harvesting and management, shifting cultivation, wood harvesting, and degradation (Arneth et al., 2017; Kondo et al., 2018b; Mitchard, 2018; Pugh et al. 2015, 2019; Williams, Gu, MacLean, Masek, & Collatz, 2016; Wolf et al., 2015), which could greatly affect regional budget estimates. For instance, a recent model that integrated the global forest age (the global forest age dataset (GFAD): Poulter et al., 2019) suggested the enhancement of CO_2 uptake (~0.45 Pg C yr^{-1}) by regrowth of northern temperate and boreal forests (Pugh et al., 2019), compared with simulations without the age information. Although this alone may not resolve the issue, enhanced uptake by the age effect appears to play a role in filling the gap between the atmospheric inversions and biosphere models in East Asia (Fig. 5), as this region is one of the hot-spots of forest regrowth (Kondo et al., 2018a). In the case of South America, incomplete representations of shifting cultivation, wood harvesting, and forest degradation are potential causes for the biosphere models being inclined towards a net sink, opposite to the results based on atmospheric inversions (Fig. 5). Currently, there is limited spatiotemporal information available regarding forest degradation, but several studies have suggested that forest degradation is more important than other processes in tropical regions, potentially accounting for twice the carbon release of deforestation (Baccini et al., 2017; Mitchard, 2018; Ryan, Berry, & Joshi, 2014). Additional sinks and sources from these processes are expected to change the patterns of hemispheric budget partitioning and corresponding regional CO_2 budgets in the biosphere models of this study. Furthermore, although the

spread in regional budget estimates was smaller within the biosphere models than the atmospheric inversions, spread in seasonality of net CO_2 flux was larger within the biosphere models than the atmospheric inversions across global, hemispheric, and regional scales (Fig. S6). Thus, we cannot conclude that biosphere models are more reliable than atmospheric inversions based on the consistency of the hemispheric budget partition and regional budget estimates among models.

A tendency for ΔC_{IM}, ΔC_{VOD}, and RECCAP results to agree more with biosphere models in estimates of regional budgets and partitioning than with atmospheric inversions may suggest that they capture common signals within the carbon cycle (Figs. 5, 6). However, we need to acknowledge the fact that carbon stock changes based on inventory measurements and VOD, as well as the statistical approaches of RECCAP have their own limitations. Both ΔC_{IM} and ΔC_{VOD} provide "forest-oriented" CO_2 budgets as available inventory data are of forests in large part and the conversion of VOD to biomass was based on an empirical relationship using ground measurements of forest biomass (Liu et al., 2015). These are considered insufficient to represent the diversity of terrestrial ecosystems, which include grasslands and croplands, and their associated carbon fluxes (King et al., 2015). Uncertainty in soil carbon stocks also affects the estimation of carbon stock changes. Even in the most extensive compilation of the inventory data, the global soil carbon stocks are likely underestimated, due to missing data of deep organic soils in ecosystems such as peatlands and mangroves (Pan et al., 2011). Despite efforts to integrate possible processes in the carbon cycle for each region, the regional CO_2 budgets from RECCAP are also influenced by the limitations in the independent CO_2 fluxes used for budget assessment, including the above-mentioned limitations in atmospheric inversions, biosphere models, and inventories. Thus, along with the modeling methods, ΔC_{IM}, ΔC_{VOD}, and the statistical approaches of RECCAP should also be improved to serve as good references for future model improvements.

In addition to the above-mentioned issues of each method, further adjustments for the definition of the net CO_2 flux could reduce the gap in budget estimates between the modeling methods. For instance, lateral transports of harvested wood carbon via export and import affect regional CO_2 budget estimates (Peters, Davis, & Andrew, 2012), which is not well addressed in current biosphere models. Also, incorporation of bottom-up pathways of CO_2 resulting from oxidation of biogenetic volatile organic compounds (BVOC), CO, CH_4 (e.g., coming from biosphere, fire and fossil fuel emissions) could improve the gap in budget estimates. Despite recent progress aimed at filling the gaps between atmospheric inversions and biosphere models, our current level of modeling and process understanding is still insufficient to implement these factors into the multi-scale CO_2 budget comparison.

6. CONCLUSIONS

The aim of this study was to detail the current status of agreement between terrestrial CO_2 budgets derived from top-down and bottom-up approaches and to provide a pathway for future improvement of these methods. With comparisons under a consistent definition of net CO_2 flux, we illustrated different levels of consistency in the CO_2 budgets of atmospheric inversions and biosphere models at the global, hemispheric, and regional scales. The overlapping distributions of hemispheric budgets, and close agreement found for some regions (i.e., North America and Southeast Asia) are good indications of progress towards reconciliation of budget estimates, therefore, increasing robustness of our knowledge. However, further improvements are required to reach a more robust regional understanding.

First, differences in budget estimates between the modeling methods for East Asia and South America need to be reduced. To accomplish this, the impacts of physiological processes that contribute to net sinks or sources (e.g., age effects on regrowth, degradation, etc.) should be further investigated using biosphere models. Second, the large variability in the regional dipole effect within atmospheric inversions needs to be reduced for them to be more comparable with the estimates of biosphere models. This requires collective effort from the inverse modeling community to identify and resolve modeling issues at regional scales (e.g., detailed experiments on transport model and inversion performance, validation of fossil fuel and biogenetic flux partitioning using $^{14}CO_2$ measurements, etc.). Given these findings, caution should be taken when interpreting regional CO_2 budgets estimated using only either atmospheric inversions or biosphere models, or individual models from these approaches, unless regional applications have been properly parameterized and benchmarked with regional observations.

The terrestrial biosphere plays a major role in mitigating CO_2 emitted by human activities (Le Quéré et al., 2018b). While the partitioning of the sink between the northern hemisphere and pantropic is increasingly better constrained, we have yet to establish confidence in the roles of global regions because of the uncertainties remaining in current models. Those uncertainties continue to limit our ability to project the mitigation potential by the terrestrial biosphere (Hoffman et al., 2014), and require continuous international and multidisciplinary efforts to resolve such as those under the umbrella of the Global Carbon Project.

Acknowledgements

This paper is a contribution to the REgional Carbon Cycle Assessment and Processes (RECCAP) under the umbrella of the Global Carbon Project. M. Kondo, P.K. Patra, K. Ichii, T. Maki, and T. Saeki acknowledge support from Environment Research and Technology Development Funds of the Environmental Restoration and Conservation Agency of Japan (no. 2-1701), P.K. Patra and J.G. Canadell from Asia-Pacific Network for Global Change Research (ARCP2011-11NMY-Patra/Canadell), P. Friedlingstein from the CRESCENDO project that received funding from the European Union's Horizon 2020 research and innovation program (no. 641816), P. Friedlingstein and S. Lienert from the CCICC project that received funding from the European Union's Horizon 2020 research and innovation program (no. 821003), A. Bastos from the European Space Agency Climate Change Initiative ESA-CCI RECCAP2 project (ESRIN/4000123002/18/I-NB), A. Arneth and P. Anthoni from the German Helmholtz Association in its ATMO programme, M. Kautz from the European Union FP7 project LUC4C (no. 603542), R. Lauerwald from the VERIFY project that received funding from the European Union's Horizon 2020 research and innovation program (no. 776186), A.K. Jain from Department of Energy (no. DE-SC0016323) and National Science Foundation: NSF (no. NSF AGS 12-43071), H. Tian from NSF (no. 1243232), and J.G. Canadell, V. Haverd, T. Ziehn from the Australian National Environmental Science Program-Earth Systems and Climate Change Hub. CLM is a part of the CESM project that is supported primarily by NSF. This material is based upon work supported by the National Center for Atmospheric Research, which is a major facility sponsored by the NSF under Cooperative Agreement No. 1852977. Computing and data storage resources, including the Cheyenne supercomputer (doi:10.5065/D6RX99HX), were provided by the Computational and Information Systems Laboratory (CISL) at NCAR. We thank all the scientists, software engineers, and administrators who contributed to the development of CESM2.

Data availability: TRENDY data are available via Profs. Stephen Sitch and Pierre Friedlingstein, Exeter University (s.a.sitch@exeter.ac.uk; p.friedlingstein@exeter.ac.uk). CAMS, CT2017, JENA inversion data are available from the web sites (CAMS: https://apps.ecmwf.int/datasets/data/cams-ghg-inversions/, CT2017: https://www.esrl.noaa.gov/gmd/ccgg/carbontracker/, JENA: http://www.bgc-jena.mpg.de/CarboScope/). ACTM, MACTM, CCAM, and GELCA CAO inversion data are available by contacting Dr. Prabir K. Patra (prabir@jamstec.go.jp). JMA inversion data are available by contacting Dr. Takashi Maki (tmaki@mri-jma.go.jp). Global above-ground biomass carbon (v1.0) is available from the web site (http://wald.anu.edu.au/data_services/data/global-above-ground-biomass-

carbon-v1-0/). Flux data of Global Carbon Project are available from the web site (https://www.globalcarbonproject.org/carbonbudget/18/data.htm).

Competing interests: The authors declare that there are no competing financial interests

REFERENCES

Arneth, A., Sitch, S., Pongratz, J., Stocker, B.D., Ciais, P., Poulter, B., ... Zaehle, S. (2017). Historical carbon dioxide emissions caused by land-use changes are possibly larger than assumed. Nature Geoscience, 10(2), 79–84. doi: 10.1038/ngeo2882

Baccini, A., Walker, W., Carvalho, L., Farina, M., Sulla-Menashe, D., & Houghton, R.A. (2017). Tropical forests are a net carbon source based on aboveground measurements of gain and loss. Science, 358(6360), 230–234. doi: 10.1126/science.aam5962

Ballantyne, A.P., Andres, R., Houghton, R., Stocker, B.D., Wanninkhof, R., Anderegg, W., ... White, J.W.C. (2015). Audit of the global carbon budget: Estimate errors and their impact on uptake uncertainty. Biogeosciences, 12(8), 2565–2584. doi: 10.5194/bg-12-2565-2015

Canadell, J.G., Ciais, P., Gurney, K., Le Quéré, C., Piao, S., Raupach, M.R., & Sabine, C.L. (2011). An international effort to quantify regional carbon fluxes. Eos Transactions American Geophysical Union, 92(10), 81–82. doi: 10.1029/2011EO100001

Cervarich, M., Shu, S., Jain, A.K., Arneth, A., Canadell, J., Friedlingstein, P., … Zeng, N. (2016). The Terrestrial Carbon budget of South and Southeast Asia. Environmental Research Letters, 11, doi:10.1088/1748-9326/11/10/105006

Ciais, P., Sabine, C., Bala, G., Bopp, L., Brovkin, V., Canadell, J., ... Thornton, P. (2013). Carbon and other biogeochemical cycles. In: T.F. Stocker, D. Qin, G.-K. Plattner, M. Tignor, S.K. Allen, J. Boschung, ... P.M. Midgley (Eds.), Climate Change 2013: The Physical Science Basis, Contribution of Working Group I to the Fifth Assessment Report of the Intergovernmental Panel on Climate Change (pp. 465–570). Cambridge: Cambridge University Press.

Ciais, P., Tan, J., Wang, X., Roedenbeck, C., Chevallier, F., Piao, S.-L., ... Tans, P. (2019). Five decades of northern land carbon uptake revealed by the interhemispheric CO_2 gradient. Nature, 568(7751), 221–225. doi: 10.1038/s41586-019-1078-6

Chevallier, F., Ciais, P., Conway, T.J., Aalto, T., Anderson, B.E., Bousquet, P., ... Worthy, D. (2010). CO_2 surface fluxes at grid point scale estimated from a global 21 year reanalysis of atmospheric measurements. Journal of Geophysical Research: Atmospheres 115, D21307. doi: 10.1029/2010JD013887

593 Friedlingstein, P., Cox, P., Betts, R., Bopp, L., von Bloh, W., Brovkind, V., ... Zeng, N. (2006). Climate-
594 carbon cycle feedback analysis: results from the C4MIP model intercomparison. Journal of Climate,
595 19, 3337–3353. doi:10.1175/JCLI3800.1

596 Food and Agriculture Organization, Global forest resources assessment 2005 (Forestry Paper 147, Food
597 and Agriculture Organization, Rome, 2006). http://www.fao.org/forest-resources-assessment/past-
598 assessments/fra-2005/en/

599 Food and Agriculture Organization, Global forest resources assessment 2010 (Forestry Paper 163, Food
600 and Agriculture Organization, Rome, 2010). http://www.fao.org/forest-resources-assessment/past-
601 assessments/fra-2010/en/

602 Gaubert, B., Stephens, B.B., Basu, S., Chevallier, F., Deng, F., Kort, E.A., ... Yin, Y. (2019). Global
603 atmospheric CO_2 inverse models converging on neutral tropical land exchange, but disagreeing on
604 fossil fuel and atmospheric growth rate. Biogeosciences, 16(1), 117–134. doi: 10.5194/bg-16-117-
605 2019

606 Guimberteau, M., Zhu, D., Maignan, F., Huang, Y., Yue, C., Dantec-Nédélec, S., ... Ciais, P. (2018)
607 ORCHIDEE-MICT (v8.4.1), a land surface model for the high latitudes: Model description and
608 validation. Geoscientific Model Development, 11(1), 121–163. doi: 10.5194/gmd-11-121-2018

609 Gurney, K.R., Law, R.M., Denning, A.S., Rayner, P.J., Baker, D., Bousquet, P., ... Yuen, C.-W. (2002).
610 Towards robust regional estimates of CO_2 sources and sinks using atmospheric transport models.
611 Nature, 415(6872), 626–630. doi: 10.1038/415626a

612 Haverd, V., Smith, B., Nieradzik, L., Briggs, P.R., Woodgate, W., Trudinger, C.M., ... Cuntz, M. (2018).
613 A new version of the CABLE land surface model (Subversion revision r4601) incorporating land
614 use and land cover change, woody vegetation demography, and a novel optimisation-based
615 approach to plant coordination of photosynthesis. Geoscientific Model Development, 11(7), 2995–
616 3026. doi: 10.5194/gmd-11-2995-2018

617 Hoffman, F.M., Randerson, J.T., Arora, V.K., Bao, Q., Cadule, P., Ji, D., ... Wu, T. (2014). Causes and
618 implications of persistent atmospheric carbon dioxide biases in Earth System Models. Journal of
619 Geophysical Research: Biogeosciences, 119(2), 141–162. doi:10.1002/2013JG002381

620 Houghton, R. A. (2007) Balancing the global carbon budget. Annual Review of Earth and Planetary
621 Science, 35, 313-347. doi:10.1146/annurev.earth.35.031306.140057

Hurtt, G., Chini, L., Sahajpal, R., Frolking, S., Calvin, K., Fujimori, S., ... Lawrence, P. (2017). Harmonization of global land-use change and management for the period 850–2100. (Online). luh.umd.edu/data.shtml

Iida, Y., Kojima, A., Takatani, Y., Nakano, T., Sugimoto, M., Midorikawa, T., Ishii, M. (2015). Trends in pCO_2 and sea-air CO_2 flux over the global open oceans for the last two decades. Journal of Oceanography, 71(6), 637–661. doi:10.1007/s10872-015-0306-4

Jacobson, A.R., Fletcher, S.E.M., Gruber, N., Sarmiento, J.L., & Gloor, M. (2007). A joint atmosphere - ocean inversion for surface fluxes of carbon dioxide: 1. Methods and global-scale fluxes. Global Biogeochemical Cycles, 21(1), GB1019. doi: 10.1029/2005GB002556

Jain, A.K., Meiyappan, P., Song, Y., & House, J.I. (2013). CO_2 emissions from land-use change affected more by nitrogen cycle, than by the choice of land-cover data. Global Change Biology, 19(9), 2893–2906. doi: doi.org/10.1111/gcb.12207

Kaula, M., Dadhwal, V.K., Mohren, G.M.J. (2009). Land use change and net C flux in Indian forests. Forest Ecology and Management, 258, 2(15), 100-108. doi:10.1016/j.foreco.2009.03.049

Kato, E., Kinoshita, T., Ito, A., Kawamiya, M., & Yamagata, Y. (2013). Evaluation of spatially explicit emission scenario of land-use change and biomass burning using a process-based biogeochemical model. Journal of Land Use Science, 8(1), 104–122. doi: 10.1080/1747423X.2011.628705

Keeling, R.F. & Manning, A.C. (2014). Studies of recent changes in atmospheric O_2 content. In: H.D. Holland & K.K. Turekian (Eds.) Treatise on Geochemistry (2nd ed.) (pp. 385–404). Amsterdam: Elsevier.

Keenan, T.F., Prentice, I.C., Canadell, J.G., Williams, C.A., Wang, H., Raupach, M., & Collatz, G.J. (2016). Recent pause in the growth rate of atmospheric CO_2 due to enhanced terrestrial carbon uptake. Nature Communications, 7, 13428. doi: 10.1038/ncomms13428

Keenan, T.F., & Williams, C.A. (2018). The terrestrial carbon sink. Annual Review of Environment and Resources, 43, 219–43. doi: 10.1146/annurev-environ-102017-030204

Keller, K.M., Lienert, S., Bozbiyik, A., Stocker, T.F., Churakova (Sidorova), O.V., Frank, D.C., ... Joos, F. (2017). 20th century changes in carbon isotopes and water-use efficiency: tree-ring-based

649 evaluation of the CLM4.5 and LPX-Bern models. Biogeosciences, 14, 2641-2673. doi:10.5194/bg-
650 14-2641-2017

651 King, A.W., Andres, R.J., Davis, K.J., Hafer, M., Hayes, D.J., Huntzinger, D.N., ... Woodall, C.W.
652 (2015). North America's net terrestrial CO_2 exchange with the atmosphere 1990–2009.
653 Biogeosciences, 12(2), 399–414. doi: 10.5194/bg-12-399-2015

654 Klein Goldewijk, K., Beusen, A., Doelman, J., & Stehfest, E. (2017). Anthropogenic land use estimates
655 for the Holocene – HYDE 3.2. Earth System Scientific Data, 9, 927–953. doi: 10.5194/essd-9-927-
656 2017

657 Kondo, M., Ichii, K., Takagi, H., & Sasakawa, M. (2015). Comparison of the data-driven top-down and
658 bottom-up global terrestrial CO_2 exchanges: GOSAT CO_2 inversion and empirical eddy flux
659 upscaling. Journal of Geophysical Research: Biogeosciences, 120(7), 1226–1245. doi: 10.1002/
660 2014JG002866

661 Kondo, M., Ichii, K., Patra, P.K., Poulter, B., Calle, L., Koven, C., ... Wiltshire, A. (2018a). Plant
662 regrowth as a driver of recent enhancement of terrestrial CO_2 uptake. Geophysical Research Letters,
663 45(10), 4820–4830. doi: 10.1029/2018GL077633

664 Kondo, M., Ichii, K., Patra, P.K., Canadell, J.G., Poulter, B., Sitch, S., ... Rödenbeck, C. (2018b). Land
665 use change and El Niño-Southern Oscillation drive decadal carbon balance shifts in Southeast Asia.
666 Nature Communications, 9, 1154. doi: 10.1038/s41467-018-03374-x

667 Krinner, G., Viovy, N., de Noblet- Ducoudré, N., Ogée, J., Polcher, J., Friedlingstein, P., ... Prentice,
668 I.C. (2005). A dynamic global vegetation model for studies of the coupled atmosphere biosphere
669 system. Global Biogeochemical Cycles, 19(1), 1–33. doi: 10.1029/2003GB002199

670 Lauerwald, R., Laruelle, G.G., Hartmann, J., Ciais, P., & Regnier, P.A.G. (2015). Spatial patterns in
671 CO_2 evasion from the global river network. Global Biogeochemical Cycles, 29(5), 534–554. doi:
672 10.1002/2014GB004941

673 Le Quéré, C., Andrew, R.M., Friedlingstein, P., Sitch, S., Pongratz, J., Manning, A.C., ... Zhu, D.
674 (2018a). Global Carbon Budget 2017. Earth System Scientific Data, 10, 405-448. doi:10.5194/essd-
675 10-405-2018

Le Quéré, C., Andrew, R.M., Friedlingstein, P., Sitch, S., Hauck, J., Pongratz, J., ... Zheng, B. (2018b). Global Carbon Budget 2018. Earth System Scientific Data, 10(4), 2141–2194. doi: 10.5194/essd-10-2141-2018

Li, W., Ciais, P., Wang, Y., Peng, S., Broquet, G., Ballantyne, A.P., ... Pongratz, J. (2016). Reducing uncertainties in decadal variability of the global carbon budget with multiple datasets. Proceedings of the National Academy of Sciences, 113(46), 13104–13108. doi: 10.1073/pnas.1603956113

Liu, Y.Y., van Dijk, A.I.J.M., de Jeu, R.A.M., Canadell, J.G., McCabe, M.F., Evans, J.P., & Wang, G. (2015). Recent reversal in loss of global terrestrial biomass. Nature Climate Change, 5(5), 470–474. doi: 10.1038/nclimate2581

Maki, T., Ikegami, M., Fujita, T., Hirahara, T., Yamada, K., Mori, K., ... Conway, T.J. (2010). New technique to analyse global distributions of CO_2 concentrations and fluxes from non-processed observational data. Tellus B: Chemical and Physical Meteorology, 62(5), 797–809. doi: 10.1111/j.1600-0889.2010.00488.x

Mayorga, E., Seitzinger, S. P., Harrison, J. A., Dumont, E., Beusen, A. H. W., Bouwmand, A. F., … Drecht, G. V. (2010). Global Nutrient Export from WaterSheds 2 (NEWS 2): Model development and implementation. Environmental Modeling & Software, 25, 837-853. doi: 10.1016/j.envsoft.2010.01.007

McGregor, J.L., & Dix, M.R. (2008). An updated description of the conformal cubic atmospheric model. In: K. Hamilton & W. Ohfuchi (Eds.) High Resolution Numerical Modeling of the Atmosphere and Ocean (pp. 51–76). Berlin: Springer.

Mitchard, E.T.A. (2018). The tropical forest carbon cycle and climate change. Nature, 559(7715), 527–534. doi: 10.1038/s41586-018-0300-2

Oleson, K.W., Lawrence, D.M., Bonan, G.B., Drewniak, B., Huang, M., Koven, C.D., … Thornton, P.E. (2013). Technical Description of Version 4.5 of the Community Land Model (CLM), National Center for Atmospheric Research Technical Note. Boulder: NCAR. doi: 10.5065/D6RR1W7M

Pan, Y., Birdsey, R.A., Fang, J., Houghton, R., Kauppi, P.E., Kurz, W.A., ... Hayes, D. (2011). A large and persistent carbon sink in the world's forests. Science, 333(6045), 988–993. doi: 10.1126/science.1201609

Patra, P. K., Takigawa, M., Watanabe, S., Chandra, N., Ishijima, K., Yamashita, Y. (2018). Improved Chemical Tracer Simulation by MIROC4.0-based Atmospheric Chemistry-Transport Model (MIROC4-ACTM). SOLA, 14, 91-96. doi:10.2151/sola.2018-016

Peters, G. P., Davis, S. J., & Andrew, R. (2012). A synthesis of carbon in international trade. Biogeosciences, 9, 3247–3276. doi: 10.5194/bg-9-3247-2012

Peters, W., Jacobson, A.R., Sweeney, C., Andrews, A.E., Conway, T.J., Masarie, K., ... Tans, P.P. (2007). An atmospheric perspective on North American carbon dioxide exchange: CarbonTracker. Proceedings of the National Academy of Sciences, 104(48), 18925–18930. doi: 10.1073/pnas.0708986104

Peylin, P., Baker, D., Sarmiento, J., Ciais, P., & Bousquet, P. (2002). Influence of transport uncertainty on annual mean and seasonal inversions of atmospheric CO_2 data. Journal of Geophysical Research, 107(D19), 4385. doi: 10.1029/2001JD000857

Peylin, P., Law, R.M., Gurney, K.R., Chevallier, F., Jacobson, A.R., Maki, T., … Zhang, X. (2013). Global atmospheric carbon budget: results from an ensemble of atmospheric CO_2 inversions. Biogeosciences, 10, 6699–6720. doi: 10.5194/bg-10-6699-2013

Poulter, B., Aragão, L., Andela, N., Bellassen, V., Ciais, P., Kato, T., ... Shivdenko, A. (2019). The Global Forest Age dataset and its uncertainties (GFADv1.1). National Aeronautics and Space Administration, PANGAEA (Online). doi: 10.1594/PANGAEA.897392

Pugh, T.A.M., Arneth, A., Olin, S., Ahlström, A., Bayer, A.D., Klein Goldewijk, K., ... Schurgers, G. (2015). Simulated carbon emissions from land-use change are substantially enhanced by accounting for agricultural management. Environmental Research Letters, 10(12), 124008. doi: 10.1088/1748-9326/10/12/124008

Pugh, T.A.M., Lindeskog, M., Smith, B., Poulter, B., Arneth, A., Haverd, V., & Calle, L. (2019). Role of forest regrowth in global carbon sink dynamics. Proceedings of the National Academy of Sciences, 116(10), 4382–4387. doi: 10.1073/pnas.1810512116

Raymond, P. A., Hartmann, J., Lauerwald, R., Sobek, S., McDonald, C., ... Guth, P. (2013). Global carbon dioxide emissions from inland waters. Nature, 503, 355–359. doi:10.1038/nature12760

Regnier, P., Friedlingstein, P., Ciais, P., Mackenzie, F.T., Gruber, N., Janssens, I.A., ... Thullner, M. (2013). Anthropogenic perturbation of the carbon fluxes from land to ocean. Nature Geoscience, 6, 597–607. doi:10.1038/ngeo1830

Rödenbeck, C., Houweling, S., Gloor, M., & Heimann, M. (2003). Time-dependent atmospheric CO_2 inversions based on interannually varying tracer transport. Tellus B: Chemical and Physical Meteorology, 55(2), 488–497. doi: 10.1034/j.1600-0889.2003.00033.x

Rödenbeck, C., Zaehle, S., Keeling, R., & Heimann, M. (2018). How does the terrestrial carbon exchange respond to inter-annual climatic variations? A quantification based on atmospheric CO_2 data. Biogeosciences, 15(8), 2481–2498. doi: 10.5194/bg-15-2481-2018

Ryan, C.M., Berry, N.J. & Joshi, N. (2014). Quantifying the causes of deforestation and degradation and creating transparent REDD+ baselines: A method and case study from central Mozambique. Applied Geography, 53, 45–54. doi: 10.1016/j.apgeog.2014.05.014

Saatchi, S.S., Harris, N.L., Brown, S., Lefsky, M., Mitchard, E.T.A., Salas, W., ... Morel, A. (2011). Benchmark map of forest carbon stocks in tropical regions across three continents. Proceedings of the National Academy of Sciences, 108(24), 9899–9904. doi: 10.1073/pnas.1019576108

Saeki, T., & Patra, P.K. (2017). Implications of overestimated anthropogenic CO_2 emissions on East Asian and global land CO_2 flux inversion. Geoscience Letters, 4(1), 9. doi: 10.1186/s40562-017-0074-7

Schimel, D., Stephens, B.B., & Fisher, J.B. (2015). Effect of increasing CO_2 on the terrestrial carbon cycle. Proceedings of the National Academy of Sciences, 112(2), 436–441. doi: 10.1073/pnas.1407302112

Schuh, A.E., Jacobson, A.R., Basu, S., Weir, B., Baker, D., Bowman, K., … Palmer, P.I. (2019) Quantifying the impact of atmospheric transport uncertainty on CO_2 surface flux estimates. Global Biogeochemical Cycles, 33(4), 484–500. doi: 10.1029/2018GB006086

Sitch, S., Smith, B., Prentice, I.C., Arneth, A., Bondeau, A., Cramer, W., ... Venevsky, S. (2003). Evaluation of ecosystem dynamics, plant geography and terrestrial carbon cycling in the LPJ dynamic vegetation model. Global Change Biology, 9(2), 161–185. doi: 10.1046/j.1365-2486.2003.00569.x

759 Sitch, S., Huntingford, C., Gedney, N., Levy, P.E., Lomas, M., Piao, S.L., ... Woodward, F.I. (2008).
760 Evaluation of the terrestrial carbon cycle, future plant geography and climate-carbon cycle
761 feedbacks using five Dynamic Global Vegetation Models (DGVMs). Global Change Biology,
762 14(9), 2015–2039. doi: 10.1111/j.1365-2486.2008.01626.x

763 Sitch, S., Friedlingstein, P., Gruber, N., Jones, S.D., Murray-Tortarolo, G., Ahlström, A., ... Myneni, R.
764 (2015). Recent trends and drivers of regional sources and sinks of carbon dioxide. Biogeosciences,
765 12(3), 653–679. doi: 10.5194/bg-12-653-2015

766 Smith, B., Wårlind, D., Arneth, A., Hickler, T., Leadley, P., Siltberg, J., & Zaehle, S. (2014).
767 Implications of incorporating N cycling and N limitations on primary production in an individual-
768 based dynamic vegetation model. Biogeosciences, 11, 2027–2054. doi: 10.5194/bg-11-2027-2014

769 Stephens, B.B., Gurney, K.R., Tans, P.P., Sweeney, C., Peters, W., Bruhwiler, L., ... Denning, A.S.
770 (2007). Weak northern and strong tropical land carbon uptake from vertical profiles of atmospheric
771 CO_2. Science, 316(5832), 1732–1735. doi: 10.1126/science.1137004

772 Thompson, R.L., Patra, P.K., Chevallier, F., Maksyutov, S., Law, R.M., Ziehn, T., … Ciais, P. (2016).
773 Top–down assessment of the Asian carbon budget since the mid 1990s. Nature Communications, 7,
774 10724. doi: 10.1038/ncomms10724

775 Tian, H., Chen, G., Lu, C., Xu, X., Hayes, D.J., Ren, W., ... Wofsy, S.C. (2015). North American
776 terrestrial CO_2 uptake largely offset by CH_4 and N_2O emissions: Toward a full accounting of the
777 greenhouse gas budget. Climatic Change, 129(3–4), 413–426. doi: 10.1007/s10584-014-1072-9

778 Viovy, N. (2018). CRUNCEP Version 7 - Atmospheric forcing data for the Community Land Model.
779 Research Data Archive at the National Center for Atmospheric Research, Computational and
780 Information Systems Laboratory (Online). http://rda.ucar.edu/datasets/ds314.3/

781 Williams, C.A., Gu, H., MacLean, R., Masek, J.G., & Collatz, J. (2016). Disturbance and the carbon
782 balance of US forests: A quantitative review of impacts from harvests, fires, insects, and droughts.
783 Global Planetary Change, 143, 66–80. doi: 10.1016/j.gloplacha.2016.06.002

784 Wolf, J., West, T.O., Le Page, Y., Kyle, G.P., Zhang, X., Collatz, G.J., & Imhoff, M.L. (2015). Biogenic
785 carbon fluxes from global agricultural production and consumption. Global Biogeochemical Cycles,
786 29(10), 1617–1639. doi: 10.1002/2015GB005119

Zhuravlev, R., Khattatov, B., Kiryushov, B., & Maksyutov, S. (2011). A novel approach to estimation of time-variable surface sources and sinks of carbon dioxide using empirical orthogonal functions and the Kalman filter. Atmospheric Chemistry and Physics, 11(20), 10305–10315. doi: 10.5194/acp-11-10305-2011

Zscheischler, J., Mahecha, M.D., Avitabile, V., Calle, L., Carvalhais, N., Ciais, P., ... Reichstein, M. (2017). Reviews and syntheses: An empirical spatiotemporal description of the global surface–atmosphere carbon fluxes: Opportunities and data limitations. Biogeosciences, 14, 3685–3703. doi: 10.5194/bg-14-3685-2017

Atmospheric inversion

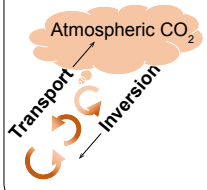

Net CO_2 flux between atmosphere and land estimated from atmospheric CO_2 measurements considering wind transport. Atmospheric inversion seeks an optimal solution from atmospheric CO_2 measurements and prior information, such as fossil fuel burning, fire emissions, and net land and ocean fluxes.

O_2-based method

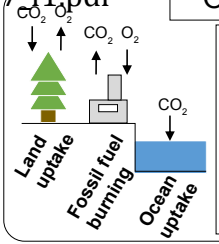

Global net land CO_2 flux based on long-term measurements of atmospheric O_2 (in terms of O_2/N_2 ratio) and CO_2. Measurement data are fed into mathematical equations for contruction and destruction of organic matters that exert the dominant control on the atmospheric O_2 and CO_2 variability.

Residual method

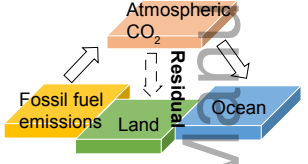

Global net land CO_2 flux estimated as a residual of the difference between measurements of CO_2 growth rate, estimations of fossil fuel emissions, and atmosphere-ocean CO_2 exchange.

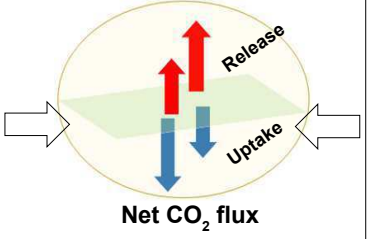

Carbon stock change

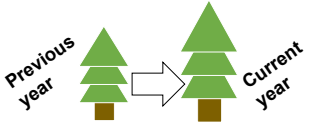

Vegetation optical depth (VOD)-based: annual carbon stock change based on successive VOD measurements from passive microwave sensors.
Inventory-based: decadal carbon stock change based on regionally aggregated inventory measurements.

Biosphere model

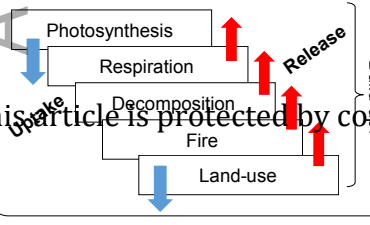

Net CO_2 flux as a sum of fluxes simulated under theoretical and semi-empirical bases. It considers processes of carbon uptake and release. Such as photosynthesis, respiration, decomposition, land-use change emissions, and fire emissions, etc.